American Journal of Chemistry 2025, 15(4): 81-88
DOI: 10.5923/j.chemistry.20251504.01

Synthesis of Glycerol Carbonate Methacrylate and Its Copolymerization with AESO

Susana Valencia Bermudez[1], Enrique Vigueras Santiago[1], Susana Hernández López[1,*], Luis Edmundo Lugo Uribe[2], Rolando Villa Moreno[2]

[1]Laboratorio de Investigación y Desarrollo de Materiales Avanzados, Facultad de Química, Universidad Autónoma del Estado de México (UAEMEX), Campus Rosedal, km 14.5 Carretera Toluca-Atlacomulco, San Cayetano de Morelos, Toluca, Estado de México, México
[2]CIATEQ, A.C. Centro de Tecnología Avanzada, Circuito de la Industria Pte Lte 11, Mza 3, No. 11. Parque Industrial Ex Hacienda Doña Rosa, Lerma, México

Abstract Glycerol carbonate methacrylate (GCMA) is a multifunctional monomer that integrates the reactivity of both cyclic carbonate and methacrylate groups, making it a promising precursor for the development of advanced polymeric materials. In this study, GCMA was synthesized through a two-step process: first, glycerol was converted into glycerol carbonate via transcarbonation with dimethyl carbonate under mild, solvent-free conditions using calcium oxide as a catalyst. Subsequently, the hydroxyl group of glycerol carbonate was functionalized with methacrylic anhydride in the presence of Amberlite IRC120H, yielding GCMA. The structure and purity of the synthesized monomer were confirmed by NMR and FTIR spectroscopy. To obtain a fully biobased polymeric material, GCMA was copolymerized with acrylate epoxidized soybean oil (AESO) at 1:1 and 2:1 molar ratio via free radical polymerization at 140 °C, without the use of any initiator. The resulting copolymers exhibit potential for sustainable applications due to their renewable origin and tunable thermal and mechanical properties.

Keywords Glycerol, Biobased polymers, Glycerol carbonate methacrylate, Carbonatation, Acrylate epoxidized soybean oil

1. Introduction

In recent years, interest in synthesizing polymers from bio-based materials has increased significantly due to the need to reduce dependence on petroleum-derived resources and the need to reduce greenhouse gas emissions.

Solutions have emerged to replace fossil fuels with more environmentally friendly renewable energies. In the transportation sector, biodiesel obtained from vegetable resources has been developed as a fuel to replace traditional petroleum-based energy. In different sectors such as biomedical, textile, automotive, packaging agriculture, and others, polylactic acid (PLA) has become one of those biopolymers with excellent potential to replace synthetic polymers. PLA's properties can be controlled, allowing its use in a variety of applications [1]. It can be manufactured from renewable resources such as corn and sugar beets, which are considered compostable and biodegradable [2].

Glycerol is widely available; in many countries, the level of diesel production has led to the production of glycerol as a byproduct of the process [3-6]. In the biodiesel industry, approximately 100 kg of glycerol is produced per ton of biodiesel. It is also a byproduct in soap saponification and propylene production. Glycerol, also known as glycerin, is chemically called propane-1,2,3-triol. It is a key material in the production of high-value bio-based molecules. Its physical and chemical properties make it a versatile organic compound; it is considered non-toxic, edible, bio sustainable, and biodegradable. [5,6]. Glycerol can be transformed into a variety of derivatives [7], including the valuable 4-hydroxymethyl-1,3- dioxolan-2-one or carbonate glycerol (CG) [5,7-10]. CG is a five-membered cyclic carbonate considered environmentally friendly and low toxicity that stands out for its physical and chemical properties, as it achieves an interesting chemical reactivity due to its two different roles of the hydroxyl group and the cyclic carbonate group, which act as a nucleophile and electrophile groups, respectively [11].

There are different synthesis routes for carbonation of glycerol, each involving numerous reactants as carbonyl sources, such as phosgene, carbon monoxide, urea, carbon dioxide, or organic carbonates [8-11]. However, some of these processes are limited by the toxicity of the reactants and the difficulty of implementing chemical reactions. The transesterification of glycerol with dialkyl carbonates is considered an environmentally benign chemical reaction [8], and also it is used industrially due to its ease, cheapness, and

* Corresponding author:
shernandezl@uaemex.mx (Susana Hernández López)
Received: Aug. 13, 2025; Accepted: Sep. 2, 2025; Published: Sep. 8, 2025
Published online at http://journal.sapub.org/chemistry

high yields when a basic and heterogeneous catalyst is employed. Even although many catalysts have been studied for this transesterification, e.g., inorganic bases [10], ionic liquids [12,13], lipases [14], and N-heterocyclic carbenes [15], heterogeneous inorganic bases are preferred for the industrial preparation of CG from glycerol and DMC, mainly based on their cost, recovery and reuse [8].

Monomers derived from glycerol, which contain a free-radical polymerizable group such as acrylate, methacrylate, allylic, or vinylic groups, along with a secondary cyclo-carbonate group, are of great interest and widely used in pharmaceutical and cosmetic applications [16-18]. Their popularity is due to their low vapor pressure, minimal flammability and toxicity, excellent biodegradability, and enhanced polarity properties. Methacrylate monomers containing cyclic carbonate have been identified having high reactivity, and also have been studied the free radical copolymerization of glycerol carbonate methacrylate. This studies showed that the carbonate group activates the double bond of the methacrylic function, making copolymerization with different acrylates such as methyl methacrylate (MMA), butyl acrylate (BA), and some other types of acrylates that can be polymerized by free radicals and have an effect on the thermomechanical properties of the generated copolymers [18].

Another important biobased acrylate monomer is the acrylate epoxidized soybean oil (AESO), Figure. 1, which is one of the commercial monomers of great interest in various industrial applications [19-22]. Some of its most important characteristics include high compatibility with polymers and low toxicity, allowing its use in medical and food applications. It is sustainable, since it is derived from renewable sources like soybean oil and it is a more environmentally friendly option compared to petroleum-based polymers. Thanks to these properties, acrylate epoxidized soybean oil is used in the production of coatings, adhesives, plasticizers, and other advanced materials. AESO-based coatings offer low toxicity, high efficiency, and environmental benefits, making them a promising alternative to petroleum-based resins.

Acrylate epoxidized soybean oil has been widely used in surface coatings to provide hydrophobicity. With the addition of acrylates, the triglyceride can react via addition polymerization. Also, it has been copolymerized with monomers derived from petroleum, such as styrene and methylmethacrylate copolymers [23,24], used in UV-curable coatings. These copolymers improve adhesion, flexibility, and thermal stability [25,26]. Other acrylate copolymers are actually developed for 3D printing resins; these copolymers offer high reactivity and durability in biomedical scaffolds.

In the present work, two copolymers derived from AESO and GCMA were prepared, and their thermal properties were compared with those of the corresponding homopolymers, Poly-AESO and PolyGCMA. With the aim of obtaining a fully biobased crosslinked polymer, the thermal copolymerization of GCMA was evaluated in the absence of solvent and initiator.

2. Materials and Methods

Powdered Calcium Carbonate, CaO_3, ACS reagent, ≥ 99%; Glycerol ≥ 99.5%; Dimethyl carbonate (DCM) ≥ 99%; Methacrylic Anhydride, AESO 1.04 g/mL at 25 ℃ (lit.), Amberlite IRC-120(H) 16-50 mesh; Dichloroethane RA, Ethyl Acetate RA, hexane RA; and Deuterated Chloroform, were all purchased from Sigma-Aldrich Co., México. The acrylate functionality of AESO and the molecular weight was determined by ^{1}H-NMR to be 2.5 acrylate groups per molecule and 1130 g/mol, respectively. Prior to use, the inhibitor in AESO was removed by passing it through a column packed with MEHQ scavenger beads.

FT-IR spectra were recorded using an IRPrestige-21 Shimadzu spectrometer equipped with a diamond crystal in horizontal attenuated total reflectance (HATR) mode. All spectra were collected in absorbance mode with 64 scans and a resolution of 4 cm^{-1}, over a wavenumber range of 560–4000 cm^{-1}.

Raman spectroscopy was performed using an Xploraplus μ-Raman spectrometer (Horiba Jobin) coupled to an Olympus microscope. The CaO sample was analyzed using 532 nm excitation, with an acquisition time of 60 s and a 10% filter.

Nuclear Magnetic Resonance (NMR) spectra were recorded on a Bruker Avance III spectrometer operating at 300 MHz, using deuterated chloroform as solvent and tetramethylsilane (TMS) as internal standard. Chemical shifts are reported in ppm. Samples were prepared by dissolving 10–20 mg of product in 0.5 mL of deuterated chloroform.

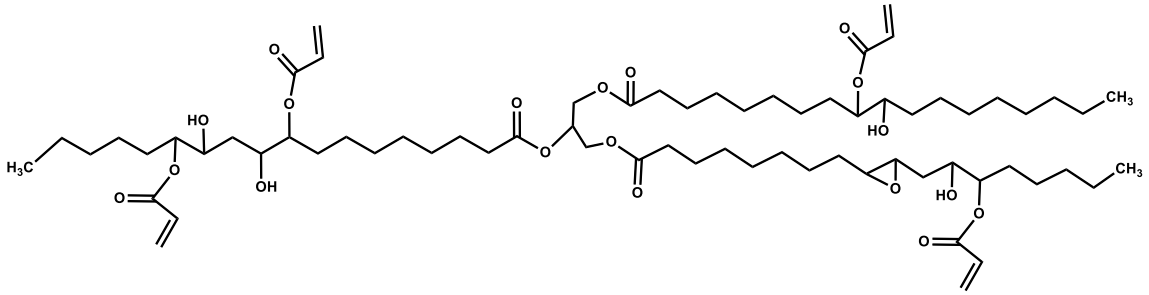

Figure 1. Acrylate epoxidized soybean oil (AESO)

Thermal analysis: DSC measurements were conducted using a TA Instruments Q20 calorimeter. Glass transition temperatures (T_g) were determined by heating 5 mg of sample from –40 to 200 ℃ under a nitrogen atmosphere at a rate of 10 ℃/min. TGA analysis was performed using a TA Instruments Q50 system, heating samples from 30 to 600 ℃ under nitrogen at 10 ℃/min, to determine the onset decomposition temperature.

X-ray diffraction (XRD) patterns were obtained using a Bruker D8 Advance diffractometer with a Cu Kα source (λ = 0.1542 nm), operating at 30 kV and 30 mA. Patterns were recorded at 25 ℃ over a 2θ range of 10–90 °, with a step size of 0.05 °.

2.1. Preparation of the CaO Catalyst

In this study, CaO was used as a basic catalyst for the carbonation reaction. CaO is among the most widely studied heterogeneous basic catalysts for transcarbonation and transesterification due to its high activity, mild reaction conditions, reusability, availability, and low cost [27].

The CaO catalyst was prepared by calcining and decomposing $CaCO_3$ in a Carbolite tubular furnace at 900 ℃ for 8 hours. After calcination, the CaO was gradually cooled inside the furnace to minimize moisture absorption from the environment.

2.2. Glycerol Carbonate (GC) Synthesis

Table 1. Carbonation Reaction Conditions

Reaction	Temperature (℃)	Catalyst/glycerol ratio (mol/mol)
1	75	0.10
2	65	0.10
3	75	0.02
4	70	0.06
5	65	0.02

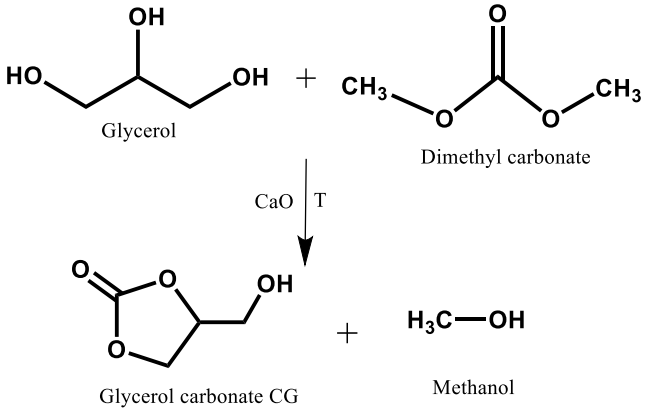

Figure 2. Transcarbonation reaction for produce CG

Glycerol was reacted with dimethyl carbonate (DMC) in the presence of CaO to produce GC (Figure. 2). To evaluate the effectiveness of the prepared CaO, the reaction conditions listed in Table 1 were adopted, based on the work [28], where yields of up to 90% were achieved using a catalyst/glycerol molar ratio of 0.06 and a DMC/glycerol molar ratio of 5 at 75 ℃ for 1.5 hours.

In our experiments, we tested reaction temperatures of 65 ℃, 70 ℃, and 75 ℃, with catalyst/glycerol molar ratios ranging from 0.02 to 0.1, while maintaining a DMC/glycerol molar ratio of 5.0. Reactions were carried out in a two-neck flask under reflux in a water bath, with magnetic stirring and no solvent.

In a typical procedure, 1 g (0.011 mol) of glycerol was added to a two-neck flask, followed by 5 mL of DMC (0.055 mol) and CaO as the catalyst. The reaction was monitored by (a) TLC using ethyl acetate as eluent, and (b) FTIR analysis, observing the decrease of OH vibration bands (3200, 1020, and 1110 cm^{-1}) from glycerol and the appearance of GC bands at 1790 and 1180 cm^{-1}, corresponding to C=O and C–O stretching vibrations of the five-membered cyclic carbonate.

After completion, the CaO catalyst was filtered, and unreacted glycerol was removed by silica column chromatography using ethyl acetate as eluent. The resulting GC was characterized by FTIR, ǂH-NMR, and thermogravimetric analysis (TGA).

2.3. Synthesis of Glycerol Carbonate Methacrylate (GCMA)

Glycerol carbonate methacrylate (GCMA, Figure. 3) was synthesized by reacting GC with methacrylic anhydride as the acrylate source.

1 g of GC (8.5 mmol) was placed in a round-bottom flask with 10 mL of dichloroethane, followed by 1.4 mL of methacrylic anhydride (10% molar excess relative to GC) and 0.03 g of Amberlite IRC-120H. As the reaction progressed, samples were taken for FTIR analysis, which showed characteristic bands of the five-membered cyclic carbonate. The band at 1790 cm^{-1} split and broadened, forming a new signal at 1740 cm^{-1}, attributed to C=O stretching of the ester group. The reaction was also monitored by TLC (ethyl acetate/hexane 35:65 v/v).

Upon completion, the Amberlite beads were filtered, and an organic–aqueous separation (5% $CaCO_3$) was performed to remove the formed methacrylic acid. The organic phase was dried with magnesium sulfate to eliminate residual water. Final purification was achieved by silica column chromatography using ethyl acetate/hexane (35:65 v/v) as eluent. GCMA was characterized by FTIR, ǂH-NMR, DSC, and TGA.

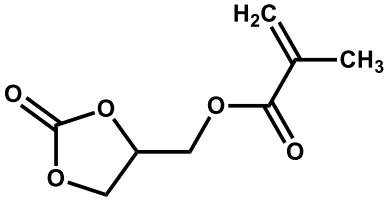

Figure 3. Glycerol carbonate methacrylate (CGA)

2.4. Polymerization of CGMA and AESO, and Copolymerización AESO:CGMA

The homopolymerization of GCMA and AESO, as well as the copolymerization of AESO:GCMA at 1:1 and 1:2 molar ratios, was carried out on a glass substrate in the absence of a free radical initiator, using a programmable oven at 140 °C. The progress of polymerization was monitored by tracking the decrease in FTIR bands corresponding to the double bonds of the acrylate groups. Upon completion of polymerization, DSC and TGA analyses were performed.

3. Results and Discussion

3.1. Characterization of CaO

The synthesized calcium oxide was characterized by Raman spectroscopy and X-ray diffraction (XRD). The Raman bands observed in the CaO spectrum (Figure. 4) can be attributed to the presence of $Ca(OH)_2$ (3614.3, 700, and 350 cm^{-1}) and $CaCO_3$ (1071 and 722 cm^{-1}), considering that pure CaO does not exhibit Raman-active modes. The formation of $Ca(OH)_2$ and $CaCO_3$ is due to hydration and carbonation of highly reactive CaO upon exposure to ambient conditions after removal from the oven [29].

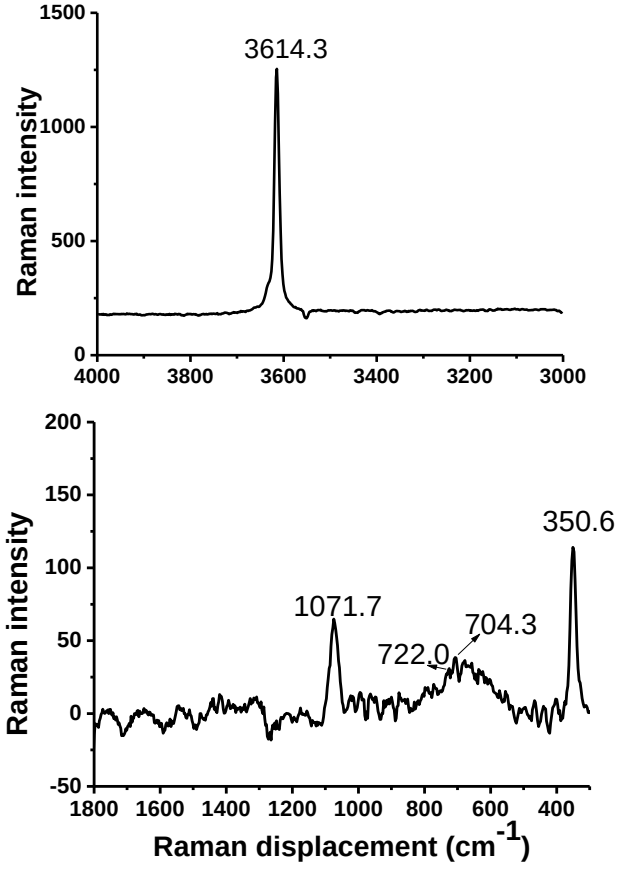

Figure 4. Raman spectroscopy of CaO

The X-ray diffraction pattern of CaO is shown in Figure. 5, confirming its face-centered cubic crystal structure, in accordance with JCPDS 9006703 from the Crystallography Open Database [30]. The diffraction peaks of CaO were observed at 2θ values of 32.2 ° (111), 37.3 ° (220), 53.8 ° (220), 64.1 °(311), 67.3 °(222), 80.8 °(400), and 88.4 °(331). Low-intensity peaks at 33.6 ° and 48.2 ° correspond to $Ca(OH)_2$.

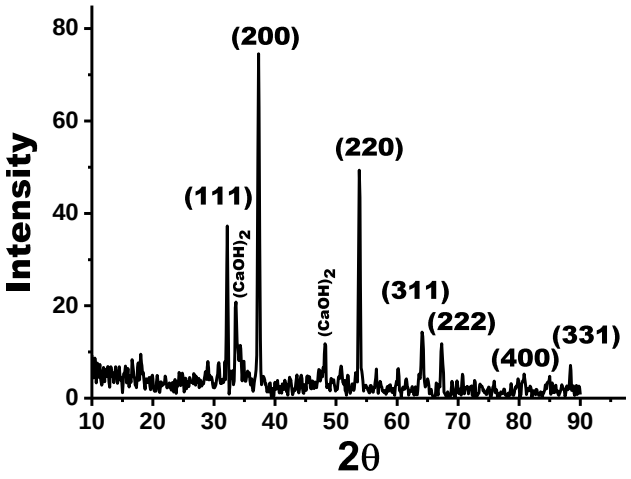

Figure 5. XRD of synthesized CaO

3.2. Characterization of Glycerol Carbonate (CG)

The results of the carbonation reactions for the synthesis of glycerol carbonate (GC) are summarized in Table 2. Under the conditions designated as Reaction RX1, the highest yield (70.9%) was achieved in 25 minutes. These conditions involved the highest reaction temperature (75 °C) and the highest catalyst/glycerol molar ratio (0.1). Reaction time was a critical factor, as slightly longer times led to polymerization of the product, resulting in an insoluble and viscous material. In contrast, Reaction RX5, which employed the lowest reaction temperature and catalyst/glycerol ratio, yielded only 36%, and required a significantly extended reaction time of approximately 10 hours.

Table 2. Carbonation reaction results

Reaction No.	Temperature (℃)	Catalyst/glycerol ratio (mol/mol)	% CG Yield	Reaction time
RX1	75	0.10	70.9	25 min
RX2	65	0.10	67.1	35 min
RX3	75	0.02	56.4	10 min.
RX4	70	0.06	61.2	65 min
RX5	65	0.02	36.0	10 h

Figure 6 presents the infrared (FTIR) spectrum of glycerol carbonate, where the characteristic functional groups are identified as follows: OH stretching vibration from the 2-hydroxyethyl chain at 3443 cm^{-1}, C=O stretching vibration of the carbonyl group in the five-membered cyclic carbonate ring at 1788 cm^{-1}. COC bond stretching at 1188 cm^{-1}, CO bond stretching at 1086 cm^{-1}. These signals are consistent with those previously reported in reference [29].

The ¹H NMR spectrum of glycerol carbonate (Figure. 7) shows the following chemical shifts: δ (ppm) = 2.8-2.84 (t, 1H, OH), 4.85-4.78 (m, 1H, CH), 4.49 (dd, 1H, OCH_2), 4.35(dd, 1H, OCH_2CH), 3.99(ddd, 1H, CH_2OH), 3.71(ddd, 1H, CH_2OH). These assignments are in agreement with [31].

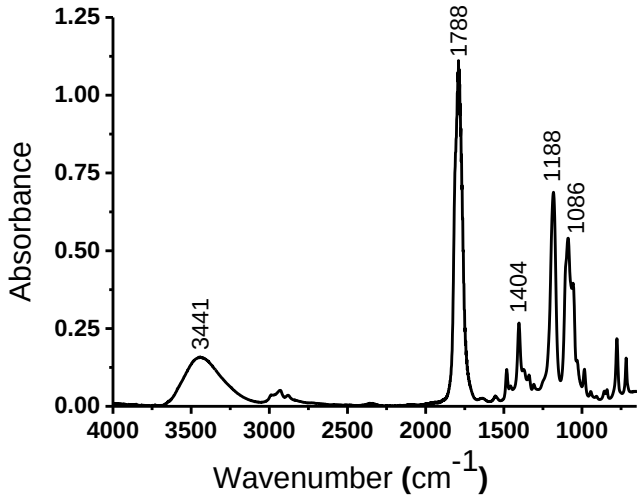

Figure 6. Glycerol carbonate FTIR spectrum

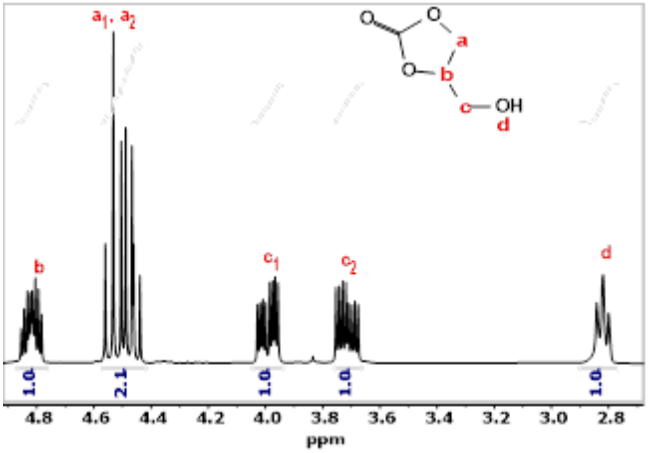

Figure 7. ^{1}H NMR of glycerol carbonate

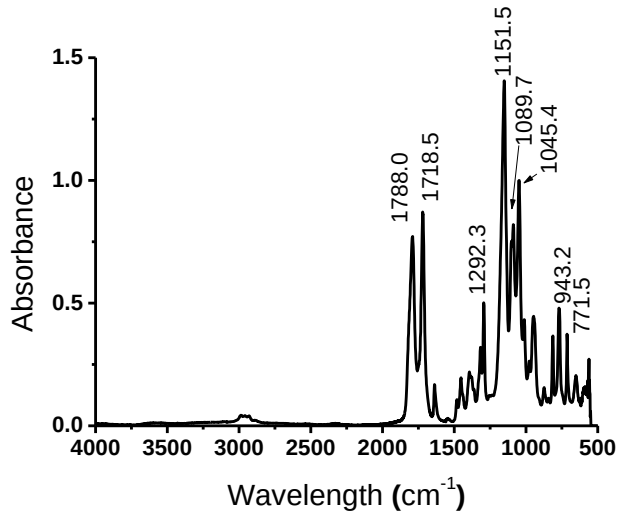

Figure 8. FTIR spectrum of GCMA

3.3. Characterization of the GCMA

Following organic-aqueous phase separation and purification via silica column chromatography, the synthesized GCMA was characterized using FTIR, TGA, and ¹H NMR spectroscopy. Figure 8 shows the FTIR spectrum of GCMA, highlighting the absorption bands corresponding to its characteristic functional groups. The vibrations that confirm the acrylation of CG include the carbonyl (C=O) stretch from methacrylic ester, observed at 1718.5 cm^{-1}. All other representative bands and their associated vibrational modes are summarized in Table 3.

Table 3. FTIR absorption assignments for GCMA

Absorption band (cm^{-1})	Vibration	Group
2931	C-H	CH_2
1788	C=O	CC5
1718.5	C=O	Ester
1640, 771	C=C	acrylate
1151.5, 1045.4	COC	CC5, ester

The ^{1}H NMR spectrum of GCMA (Figure 9) shows the following signals: ^{1}H NMR (300 MHz, $CDCl_3$) δ 6.2 (q, J = 1.1 Hz, $1H_d$), 5.67 (q, J = 1.6 Hz, $1H_d$), 5.0 (dddd, J = 8.7, 5.6, 3.9, 3.1 Hz, $1H_b$), 4.57 (t, J = 8.6 Hz, $1H_c$), 4.44 (dd, J = 12.6, 3.2 Hz, $1H_c$), 4.40–4.28 (dd, 1H; m, $1H_a$), 1.96 (t, J = 1.3 Hz, $3H_f$). This analysis confirms the successful synthesis of GCMA, as reported in [32].

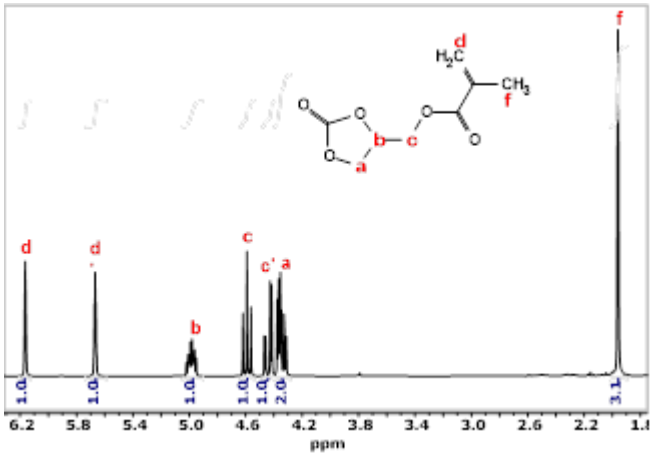

Figure 9. ^{1}H NMR of GCMA

A thermal analysis of GCMA was performed using DSC, revealing an onset temperature of 125 °C and a peak temperature of 163 °C for the exothermic polymerization curve in the absence of a catalyst. Thermogravimetric analysis (TGA), shown in Figure. 10, was conducted to compare the initial degradation temperatures (onset). The results indicate that glycerol degrades at 210 °C, CG at 231 °C, and GCMA at 269 °C, demonstrating that GCMA exhibits greater thermal stability than its precursors. As discussed in [33], during the pyrolysis of certain CG derivatives, the C–C and C–O bonds of the five-membered cyclic carbonate ring preferentially break, producing volatile

carbonates and CO_2. Subsequently, the adjacent C–O bond in esters (as in the case of GCMA) continues to degrade, generating additional fragments. This ester bond is absent in CG, which explains its lower decomposition temperature compared to GCMA. In the case of glycerol, the C–C, C–O, and O–H bonds break in a single step, forming water, formaldehyde, and acetaldehyde [34].

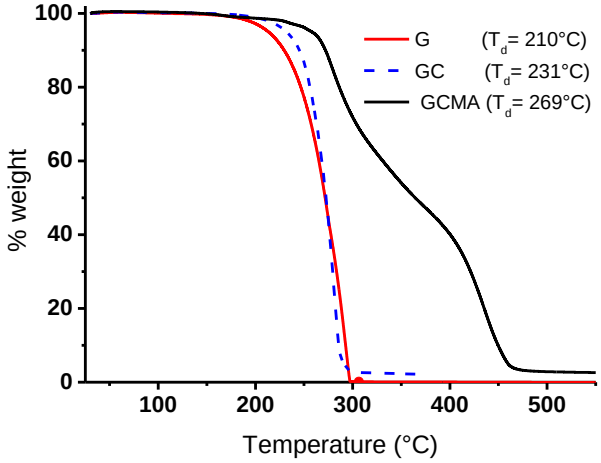

Figure 10. TGA thermogram of GCMA, CG and G (glycerol)

DSC thermograms in Figure. 11 show the polymerization exotherm curves for GCMA and for the AESO:GCMA mixtures. All curves exhibit an onset around 120 °C, with peak temperatures at 140 °C and 145 °C for the 1:2 and 1:1 mixtures, respectively; and 163 °C for GCMA. The temperature of 140 °C (indicated by the blue dotted line) falls within the polymerization range for all three samples. The main difference observed during polymerization was the time required to achieve complete crosslinking: 40 min for GCMA, 2 hr for the 1:1 mixture, 30 minutes for the 1:2 mixture, and 2 hr for AESO. This was corroborated by the disappearance of FTIR bands associated with the acrylic group, as well as by the absence of the exothermic peak in a subsequent DSC scan of the polymerized products.

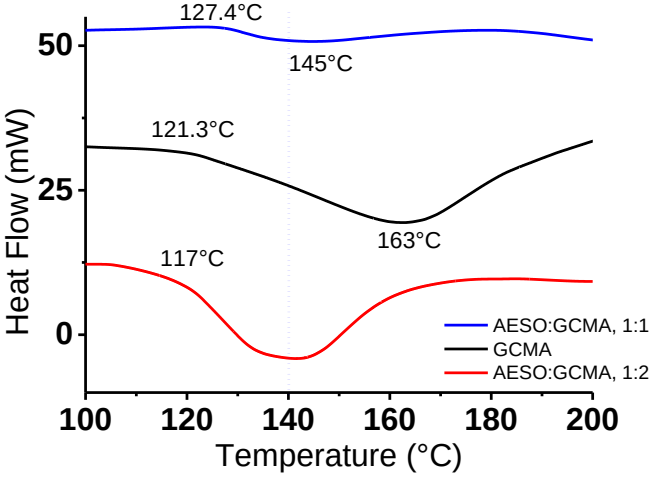

Figure 11. DSC exotherm curves for GCMA and the mixtures AESO:GCMA, 1:1 and 1:2 molar ratios

3.4. Thermal Analysis of Homopolymers and Copolymers AESO/GCMA

PolyAESO was obtained as a flexible, transparent yellow film, whereas PolyGCMA formed a transparent but brittle and inflexible film. The homopolymers of GCMA and AESO were pale and inflexible, though less brittle than PolyGCMA.

To determine the glass transition temperature (T_g), the homopolymers and copolymers of AESO-co-GCMA (in molar ratios of 1:1 and 1:2) were analyzed by DSC (Figure 12). The thermograms revealed T_g values of 9 °C for PolyAESO and 65 °C for PolyGCMA. These results are consistent with the molecular structure: AESO contains long, flexible alkyl spacers, which contribute to its lower T_g. For the copolymers, the presence of rigid cyclic carbonate and methacrylate groups led to an increase in T_g compared to AESO alone. As expected, the copolymer with a higher GCMA content exhibited a higher Tg: 14.9 °C for the 1:1 AESO-co-GCMA and 18.8 °C for the 1:2 AESO-co-GCMA.

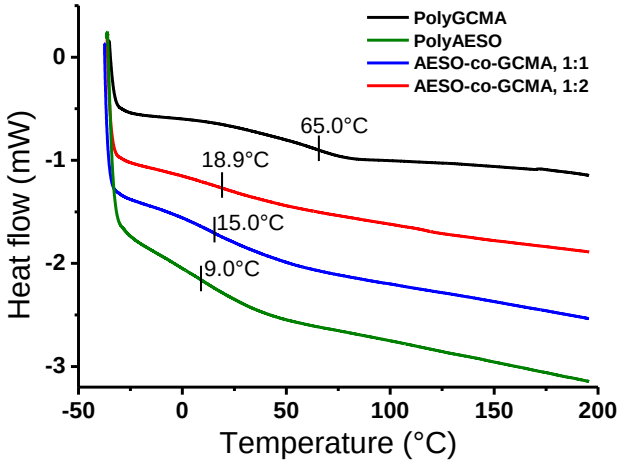

Figure 12. DSC of homopolymers and copolymers AESO-co-GCMA

Figure. 13 presents the TGA curves for the homopolymers and copolymers. The onset decomposition temperatures show the following behavior: PolyAESO, 346.8 °C; PolyGCMA, 230 °C; AESO-co-GCMA 1:1, 342 °C; and AESO-co-GCMA 1:2, 332 °C. As anticipated, the copolymers exhibit intermediate thermal stability, closer to that of PolyAESO. This is attributed to the dominant structural stability of the soybean oil-derived AESO, compared to the five-membered cyclic carbonate in GCMA, which undergoes ring opening and subsequent decomposition upon heating.

The enhanced thermal stability of the copolymers can be attributed to the crosslinked architecture introduced by AESO, which features long fatty acid chains anchored to a stable central triester core. This robust structure promotes resistance to thermal degradation. In contrast, GCMA forms a linear polymer with a pendant cyclic carbonate group and simple ester bonds along the main chain-structural elements that closely resemble its monomer and contribute to its lower thermal stability [35]. Upon copolymerization, the presence of AESO drives the formation of a three-dimensional crosslinked network, which dominates the thermal behavior

of the resulting material. As a result, the copolymers exhibit thermal properties more similar to AESO than to GCMA, reflecting the influence of AESO's stable and reticulated molecular framework.

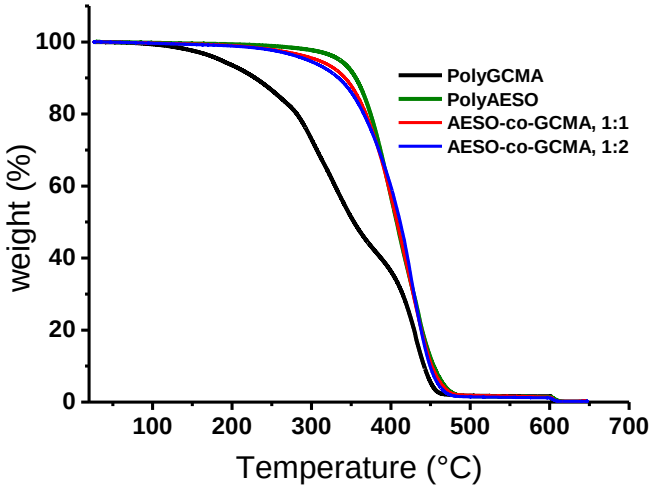

Figure 13. TGA of homopolymers and copolymers AESO-co-GCMA

4. Conclusions

GCMA is a monomer that can be polymerized without the need for catalysts, yielding a rigid, and lustrous polymer. In contrast, homopolymerization of AESO at 140 °C results in a amber-colored material with low stiffness and a glass transition temperature (T_g) of only 9 °C. However, when AESO and GCMA are copolymerized at the same temperature, increasing the proportion of GCMA significantly enhances the rigidity of the resulting copolymer and raises its T_g. For instance, a 1:2 molar ratio of AESO to GCMA produces a copolymer with a T_g of 18.9 °C. Although this represents an improvement over pure AESO, the GCMA homopolymer still exhibits far superior stiffness, with a T_g of 65 °C.

Moreover, AESO-co-GCMA polymers form crosslinked networks whose three-dimensional architecture contributes to enhanced thermal stability. This structure is primarily attributed to AESO's central triester core and long fatty acid chains. These findings demonstrate that AESO-GCMA copolymerization enables the design of materials with tunable thermal and mechanical properties, combining the renewable origin and flexibility of AESO with the structural rigidity of GCMA. Given their stability and stiffness, these copolymers represent a promising platform for the development of thermoset coatings, sustainable plastics, and advanced functional materials. Future research could explore their chemical resistance, environmental degradation behavior, and adaptability to specific industrial applications.

ACKNOWLEDGEMENTS

We gratefully acknowledge the support of CONACYT through the scholarship granted during the Ph.D. program in Materials Science at UAEMEX. The authors thank to M.C. María de las Nieves Zavala from CCIQS (SHL-2018), UAEM-UNAM, for providing technical support with NMR measurements. This work was supported by CONACyT (grant no. A1-S-33899), México.

REFERENCES

[1] S. Ahmed, S. Ikram, S. Kanchi, and K. Bisetty Ed., Biocomposites: Biomedical and Environmental Applications, New York, USA: Jenny Stanford Publishing, 2018. https://doi.org/10.1201/9781315110806.

[2] Garlotta, D., 2001, A literature review of poly (lactic acid),, Journal of Polymers and the Environment, 9, 63–84. https://doi.org/10.1023/A:1020200822435.

[3] Chilakamarry, C.R., Sakinah, A.M.M., Zularisam, A.W. et al., 2021, Glycerol waste to value added products and its potential applications., Systems Microbiology and Biomanufacturing, 1, 378–396. https://doi.org/10.1007/s43393-021-00036-w.

[4] Liu, Y., Zhong, B., and Lawal, A., 2022, Recovery and utilization of crude glycerol, a biodiesel byproduct., RSC Advances, 12, 27997. DOI: 10.1039/d2ra05090k.

[5] Das, A., Kodgire, P., Li, H., Basumatary, S., Baskar, G., and Lalthazuala Rokhum, S., 2023, Recent Advances in Conversion of Glycerol: A Byproduct of Biodiesel Production to Glycerol Carbonate., Journal of Chemistry, 2023, 8730221, 36 pages. https://doi.org/10.1155/2023/8730221.

[6] Elsayed, M., Eraky, M., Osman, A.I., Wang, J., Farghali, M., Rashwan, A.K., Yacoub, I.H., Hanelt, D., and Abomohra, A., 2024, Sustainable valorization of waste glycerol into bioethanol and biodiesel through biocircular approaches: a Review., Environmental Chemistry Letters, 22, 609–634. https://doi.org/10.1007/s10311-023-01671-6.

[7] Goyal, S., Hernández, N.B., and Cochran, E.W., 2020, An update on the future prospects pf glycerol polymers., Polymer International, 70, 911-917. DOI 10.1002/pi.6209.

[8] Fiorani, G., Perosa, A., and Selva, M., 2017, Dimethyl carbonate: A versatile reagent for a Sustainable valorization of renewables., Green Chemistry, 2018, 20, 288-322. https://doi.org/10.1039/C7GC02118F.

[9] Usman, M., Rehman, A., Saleem, F., Abbas, A., Eze, V.C., and Harvey, A., 2023, Synthesis of cyclic carbonates from CO2 cycloaddition to bio-based epoxides and glycerol: an overview of recent development., RSC Advances, 13, 22717. https://doi.org/10.1039/D3RA03028H.

[10] Saouza Junior, R.L., Eira, L.C., Detoni, Ch., and Souza, M.M.V.M., 2024, Glycerol carbonate production via transesterification: the effect of support porosity and catalyst basicity., Process, 12, 2256, 20 pp. https://doi.org/10.3390/pr12102256.

[11] Clements, J.H., 2003, Reactive applications of cyclic alkylene carbonates., Industrial & Engineering Chemistry Research, 42(4), 663-674. https://doi.org/10.1021/ie020678i.

[12] Munshi, M.K., Gade, S.M., Rane, V.H., and Kelkar, A.A., 2014, Role of cation-anion cooperation in the selective synthesis of glycidol from glycerol using DABCO-DMC ionic liquid as catalyst., RSC Advances, 4(61), 32127-32133.

DOI: 10.1039/c4ra04290e.

[13] Selva, M., Perosa, A., Guidi, S., and Cattelan, L., 2016, Ionic liquids as transesterification catalysts: applications for the synthesis of linear and cyclic organic carbonates., Beilstein Journal of Organic Chemistry, 12, 1911-1924. https://doi.org/10.3762/bjoc.12.181.

[14] Kim, S. C., Kim, Y. H., Lee, H., Yoon, D. Y., and Song, B. K., 2007, Lipase-catalyzed synthesis of glycerol carbonate from renewable glycerol and dimethyl carbonate through transesterification., Journal of Molecular Catalysis B: Enzymatic, 49, 75–78. doi: https://doi.org/10.1016/j.molcatb.2007.08.007.

[15] Hervert, B., McCarthy, P. D., and Palencia, H. 2014, Room temperature synthesis of glycerol carbonate catalyzed by N-heterocyclic carbenes., Tetrahedron Letters, 55, 133–136. doi: https://doi.org/10.1016/j.tetlet.2013.10.135.

[16] Pham, P.D., Monge, S., Lapinte, V., Raoul, Y., and Robin, J.J., 2013, Various radical polymerizations of glycerol-based monomers., European Journal of Lipid Science and Technology, 115, 28–40. DOI: 10.1002/ejlt.201200202.

[17] Rodriguez Herrero, Y., and Ullah, A., 2021, Rapid, Metal-Free, Catalytic Conversion of Glycerol to Allyl Monomers and Polymers., ACS Sustainable Chemistry and Engineering, 9, 9474−9485. https://doi.org/10.1021/acssuschemeng.1c03134.

[18] Ventura-Hunter, C., Lechuga-Islas, V.D., Ulbrich, J., Kellner, C., Schubert, U.S., Saldívar-Guerra, E., Rosales-Guzmán, M., and Guerrero-Sánchez, C., 2022, Glycerol methacrylate- based copolymers: Reactivity ratios, physicochemical characterization and cytotoxicity., European Polymer Journal, 178, 111478, 12 pp. https://doi.org/10.1016/j.eurpolymj.2022. 111478.

[19] Beach, E.S., Cui, Z., Anastas, P.T., Zhan, M., and Wool, R.P., 2021, Properties of thermosets derived from chemically modified triglycerides and bio-based comonomers., Applied Science, 3, 684-693. https://doi.org/10.3390/app3040684.

[20] Quirino, R.L., Monroe, K., Fleischer III, C.H., Biswas, E., and Kessler, M.R., 2021, Thermosetting polymers from renewable sources., Polymer International, 70(2), 167–180. https://doi.org/10.1002/pi.6132.

[21] Singhal, P., Kumar, A., Kumar, H., Kumar, V., and Vishnoi, R., 2022, Polymeric Material from Plant Oil and Their Application. In: Baskar, C., Ramakrishna, S., Daniela La Rosa, A. (eds) Encyclopedia of Green Materials. Springer, Singapore. https://doi.org/10.1007/978-981-16-4921-9_120-1.

[22] W. Liu, T. Chen, and R. Qiu, "Soybean oil-based polymers and their composites"., in Green Chemistry and Green Materials from Plant Oils and Natural Acids, ed. Z. Liu and G. Kraus, Royal Society of Chemistry, 2023, vol. 83, ch. 3, pp. 42-58. https://doi.org/10.1039/BK9781837671595-00042.

[23] S. Hernández López, and E. Vigueras Santiago., 2013, "Acrylated-epoxidized soybean oil-based polymers and their use in the generation of electrically conductive"., in Soybean: Bio-Active Compounds, H. El-Shemy ed., Ch. 11., 231. http://dx.doi.org/10.5772/52992.

[24] Lin, F-Y, Hohmann, H.D., Hernandez, N., Shen, L., Dietrich, H., and Cochran, E.W., 2020, Self-assembly of poly(styrene-*block*-acrylated epoxidized soybean oil) star-brush-like block copolymers., Macromolecules, 53(18) 8095–8107. https://doi.org/10.1021/acs.macromol.0c00441.

[25] Kumar, V., Khan, A., and Rabnawaz, M., 2023, A plant oil-based eco-friendly approach for paper coatings and their packaging applications., Progress in Organic Coatings, 176, 107386. https://doi.org/10.1016/j.porgcoat.2022.107386.

[26] Gapsari, F., Wijatmiko, I., Andoko, A., Diharjo, K., Mavinkere Rangappa, S., and Siengchin, S., 2024, Modification on fiber from alkali treatment and AESO coating to enhance UV-light and water absorption resistance in kapok fiber reinforced polyester composites., Journal of Natural Fibers, 21, 2383970. https://doi.org/10.1080/15440478.2024.2383970.

[27] Kumar, A., Some, D.K., and Kiriamiti, K.H., 2014, Pretreatment of CaO catalyst for transesterification of croton megalocarpus oil., Journal of Sustainable Research in Engineering, 1(2), 57-62. https://jsre.jkuat.ac.ke/index.php/jsre/article/view/17.

[28] Ochoa-Gómez, J.R., Gómez-Jiménez-Aberasturi, O., Maestro-Madurga, B., Pesquera-Rodríguez, A., Ramírez-López, C., Lorenzo-Ibarreta, L., Torrecilla-Soria, J., and Villarán-Velasco, M.C., 2009, Synthesis of glycerol carbonate from glycerol and dimethyl carbonate by transesterification: Catalyst screening and reaction optimization., Applied Catalysis A: General, 366 (2), 315–324. doi: 10.1016/J.APCATA.2009.07.020.

[29] Calvino-Casilda, V., Mul, G., Fernández, J.F., Rubio-Marcos, F., and Bañares, M.A., 2011, Monitoring the catalytic synthesis of glycerol carbonate by real-time attenuated total reflection FTIR spectroscopy., Applied Catalysis A: General, 409–410, 106-112. https://doi.org/10.1016/j.apcata.2011.09.036.

[30] Fiquet, G., Richet, P., and Montagnac, G., 1999, Crystal structure data from: High-temperature thermal expansion of lime, periclase, corundum and spinel Sample: PtRh10% heating wire, T = 1222 K., Physics and Chemistry of Minerals, 27,103 - 111. https://www.crystallography.net/9006695.html.

[31] Kaur, A., Prakash, R., and Ali, A., 2018, 1H NMR assisted quantification of glycerol carbonate in the mixture of glycerol and glycerol carbonate., Talanta, 178, 1001-1005. http://dx.doi.org/10.1016/j.talanta.2017.08.103.

[32] Camara, F., Caillol, S., and Boutevin, B., 2014, Free radical polymerization study of glycerin carbonate methacrylate for the synthesis of cyclic carbonate functionalized polymers., European Polymer Journal, 61, 133-144. https://doi.org/10.1016/j.eurpolymj.2014.10.001.

[33] Li, R., Liu, J., Tao, H., Sun, D., Xiao, D., Liu, Ch., 2016, The investigation of thermal pyrolysis of glycerol carbonate derivatives by TG–FTIR., Thermochimica Acta, 624, 76-81. https://doi.org/10.1016/j.tca.2015.12.002.

[34] Zhang, D., Cao, Y., Zhang, P., Liang, J., Xue, K., Xia, Y., and Qi, Z., 2021, Investigation of the thermal decomposition mechanism of glycerol: the combination of a theoretical study based on the Minnesota functional and experimental support., Phys. Chem. Chem. Phys., 26(36), 20466-20477. DOI: 10.1039/D1CP01526E.

[35] Britz, J., Meyer, W.H., and Wegner, G., 2007, Blends of Poly(meth)acrylates with 2-Oxo-(1,3)dioxolane Side Chains and Lithium Salts as Lithium Ion Conductors., Macromolecules, 40(21), 7558-7565. https://doi.org/10.1021/ma0714619.